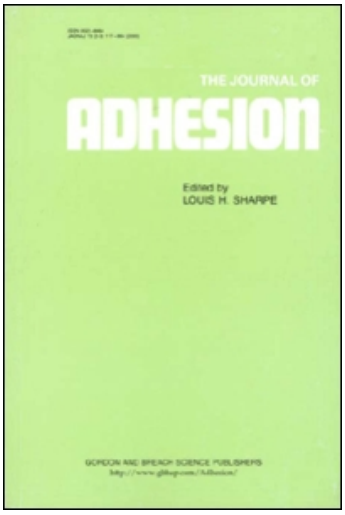

The Journal of Adhesion
Publication details, including instructions for authors and subscription information:
http://www.informaworld.com/smpp/title~content=t713453635

Cohesive zone models and the plastically deforming peel test

I. Georgiou[a]; H. Hadavinia[a]; A. Ivankovic[a]; A. J. Kinloch[a]; V. Tropsa[a]; J. G. Williams[a]
[a] Department of Mechanical Engineering, Imperial College of Science, Technology and Medicine, London, United Kingdom

Online publication date: 08 September 2010

To cite this Article Georgiou, I. , Hadavinia, H. , Ivankovic, A. , Kinloch, A. J. , Tropsa, V. and Williams, J. G.(2003) 'Cohesive zone models and the plastically deforming peel test', The Journal of Adhesion, 79: 3, 239 — 265
To link to this Article: DOI: 10.1080/00218460309555
URL: http://dx.doi.org/10.1080/00218460309555

The Journal of Adhesion, 79: 239–265, 2003

0021-8464/03 $12.00 +.00
DOI: 10.1080/00218460390148121

Taylor & Francis
Taylor & Francis Group

COHESIVE ZONE MODELS AND THE PLASTICALLY DEFORMING PEEL TEST

I. Georgiou
H. Hadavinia
A. Ivankovic
A. J. Kinloch
V. Tropsa
J. G. Williams
Department of Mechanical Engineering,
Imperial College of Science, Technology and Medicine,
London, United Kingdom

The peel test is a popular test method for measuring the peeling energy between flexible laminates. However, when plastic deformation occurs in the peel arm(s) the determination of the true adhesive fracture energy, G_c, from the measured peel load is far from straightforward. Two different methods of approaching this problem have been reported in recently published papers, namely: (a) a simple linear-elastic stiffness approach, and (b) a critical, limiting maximum stress, σ_{max}, approach. In the present article, these approaches will be explored and contrasted. Our aims include trying to identify the physical meaning, if any, of the parameter σ_{max} and deciding which is the better approach for defining fracture when suitable definitive experiments are undertaken.

Keywords: Cohesive zone models; Fracture mechanics; Laminates; Peel tests; Plastic deformation

INTRODUCTION

The peel test is a popular test method for measuring the peeling energy between flexible laminates [1–3]. The simple single-arm form is shown in Figure 1a, and the T-peel variant is illustrated in Figure 1b.

Received 28 June 2002; in final form 16 August 2002.
The authors would like to thank the EPSRC for financial support.
Address correspondence to A. J. Kinloch, Department of Mechanical Engineering, Imperial College of Science, Technology and Medicine, Exhibition Road, London SW7 2BX, UK. E-mail: a.kinloch@ic.ac.uk

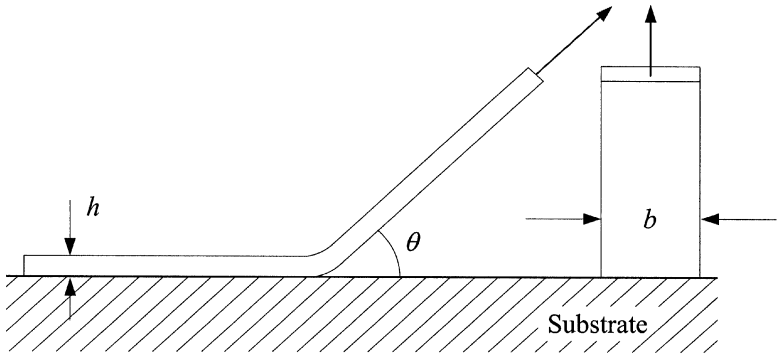

a) Single-arm peel test

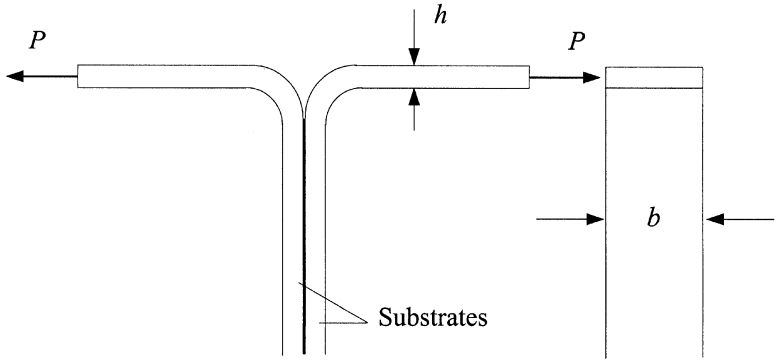

b) 'T-Peel' test

FIGURE 1 Common peel test geometries. (a) Single-arm peel test, (b) T-peel test.

For the former test method, the total energy input, G, is related to the applied steady-state peel load, P, the width, b, of the specimen and the peel angle, θ, by

$$G = \frac{P}{b}(1 - \cos\theta), \tag{1}$$

and for the T-peel we essentially have two such specimens "back-to-back," each with $\theta = \frac{\pi}{2}$, such that

$$G = \frac{2P}{b}. \tag{2}$$

This value of G includes the adhesive fracture energy, G_c, and any plastic work done in bending the peeling arm(s). The value of the adhesive fracture energy, G_c, is assumed to be a "characteristic" property of the adhesive, or interface, and ideally independent of geometrical details of the peel test such as the thickness, h, of the peel arm and the peel angle, θ. However, the value of G_c would, of course, be expected typically to be dependent upon the test rate and temperature, since we are dealing with viscoelastic materials.

When only elastic deformation occurs in the peeling arm there is no energy dissipation, so that $G = G_c$. However, in many cases, there is a rather complex bending and unbending process, as shown, for $\theta = \frac{\pi}{2}$ in Figure 2a where the peeling arm is initially bent and then gradually straightened as the peeling proceeds. A schematic diagram of the bending moment, M/b, per unit width in the peel arm and the inverse of the local radius, $1/R$, of curvature at the peel front is shown in Figure 2b and the area under the curve is the plastic-energy dissipated in bending. When a nonwork hardening material is used for the peel arm, the moments tend to the plastic limit,

$$\frac{M_p}{b} = \frac{\sigma_y h^2}{4}, \tag{3}$$

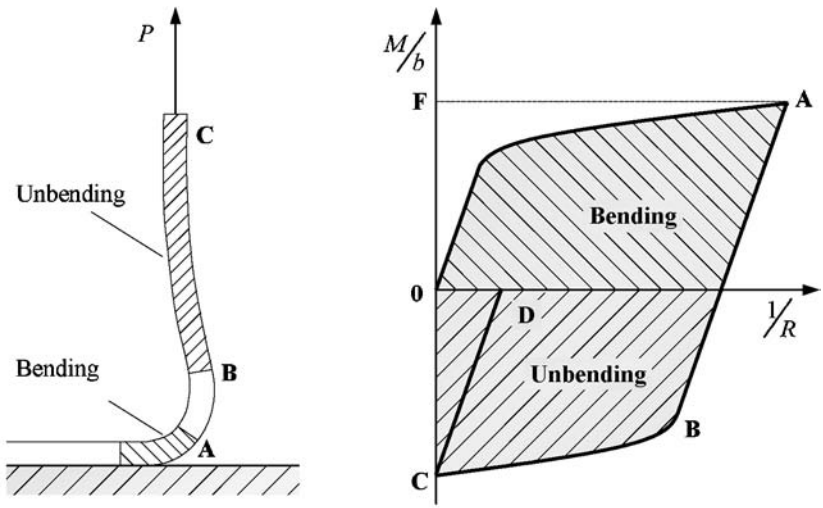

FIGURE 2 Plastic deformation. (a) 90° peel test, (b) moment-curvature diagram.

where M_p is the fully plastic moment, σ_y is the yield stress, and h is the thickness of the peel arm, and for large values of the plastic-energy dissipation:

$$G \approx 2\frac{M_p}{b} \cdot \frac{1}{R} = \frac{\sigma_y h^2}{2R}. \tag{4}$$

A crucial factor in the analysis is the root rotation, θ_o, illustrated in Figure 3. This arises from stretching of the substrate peeling arm before it debonds and reduces the plastic work done such that the proportion of G going into plastic work, G_d, is [1]

$$G_d = \frac{P}{b}[1 - \cos(\theta - \theta_o)], \tag{5}$$

i.e., for $\theta = \theta_o, G_d = 0$, and for $\theta_o = 0, G_d = G$.

Considering now only the 90° peel test, and assuming θ_o to be small, then

$$G_d = \frac{P}{b}[1 - \theta_o], \tag{6}$$

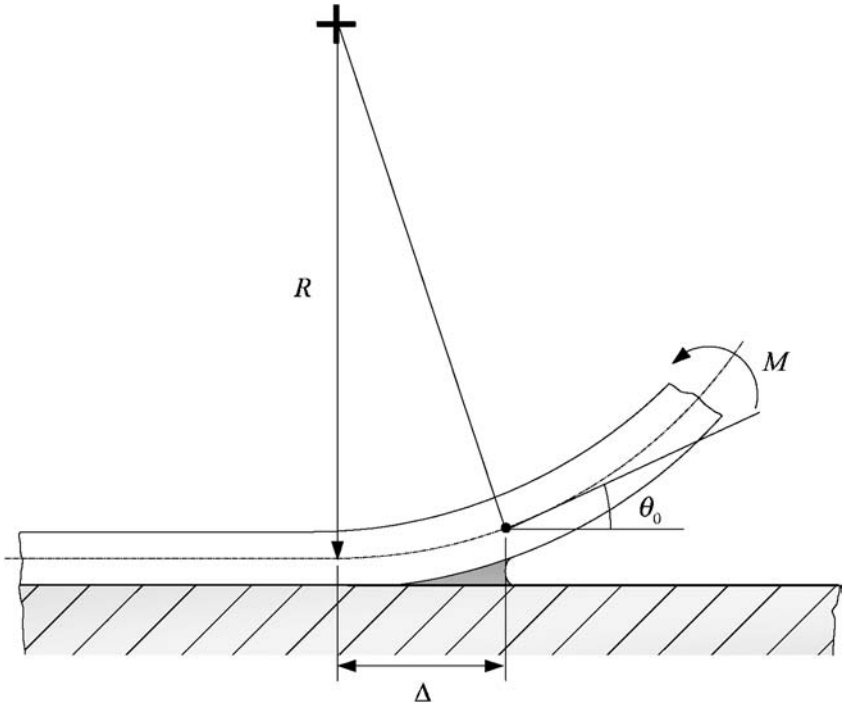

FIGURE 3 Root rotation.

and the true adhesive fracture energy, G_c, is approximately given by

$$G_c = [G - G_d] + \frac{\sigma_y^2 h}{2E} = \theta_o G + \frac{\sigma_y^2 h}{2E}, \tag{7}$$

where the term $\frac{\sigma_y^2 h}{2E}$ is the elastic energy release rate from the beam at $M = M_p$.

The value of θ_o is determined by the characteristic length of the deformation, Δ, as shown in Figure 3, and is given by

$$\theta_o = \frac{\Delta}{R}, \tag{8}$$

and on substituting into Equation (7), using Equation (4) we have

$$G_c = \left(\frac{\Delta}{h}\right) \cdot \frac{2G^2}{\sigma_y h} + \frac{\sigma_y^2 h}{2E}. \tag{9}$$

This is an approximate form but illustrates the importance of the characteristic length of the deformation, Δ. More detailed analyses of the plastic- and elastic-deformations, for both bilinear and power-law work hardening peel arms, have been given elsewhere [1, 3] but are, in essence, versions of Equation (9). However, these more detailed analyses are in the form of simultaneous nonlinear equations which require numerical solutions. These solutions will be discussed later, together with the various forms of Δ.

There are two different approaches for ascertaining the value of Δ: (a) the linear-elastic stiffness approach, and (b) the critical, limiting maximum stress, $\sigma_{\max}$, approach. In the present paper, these approaches will be explored and contrasted. Our aims include trying to identify the physical meaning, if any, of the parameter $\sigma_{\max}$ and deciding which is the better approach for defining fracture, when suitable definitive experiments are undertaken.

THE DETERMINATION OF Δ

The Linear-Elastic Stiffness Approach

The most common solution for Δ comes from the beam on a linear-elastic foundation approach which assumes a stiffness of k_s such that the stress, σ, *versus* displacement, u, relationship for the cohesive zone at the crack tip is as shown in Figure 4a [1, 5]. For this case

$$\left(\frac{\Delta}{h}\right)^4 = \frac{E}{3h}\left(\frac{b}{k_s}\right), \tag{10}$$

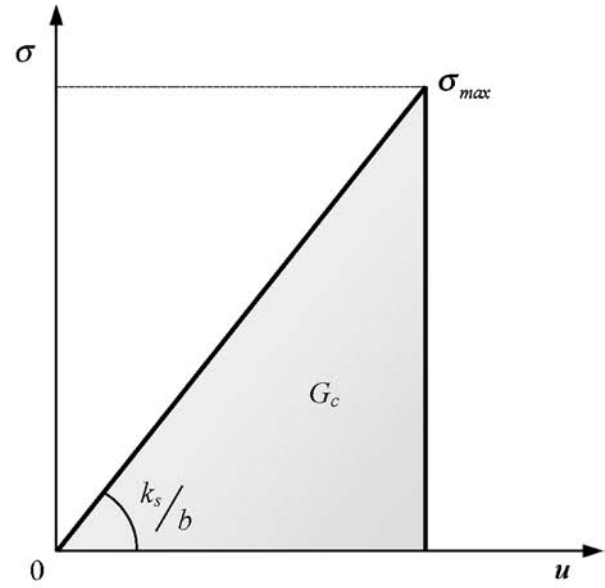

a) Linear stiffness curve

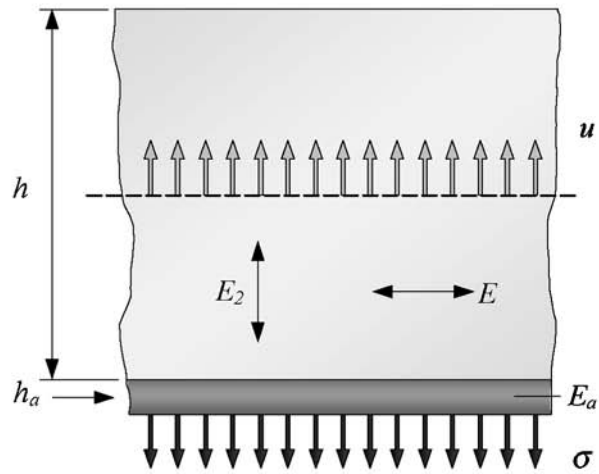

b) Stiffness factors

FIGURE 4 Linear-elastic stiffness approach. (a) Linear stiffness curve, (b) stiffness factors.

and k_s may be calculated for half the beam thickness and an adhesive layer, as shown in Figure 4b. For the combined stiffness of a peel arm of thickness $\frac{h}{2}$ (with a transverse modulus E_2) and an adhesive layer of thickness h_a (and modulus E_a) we have

$$\frac{b}{k_s} = \frac{h}{2E_2} + \frac{h_a}{E_a},$$

and hence:

$$\left(\frac{\Delta}{h}\right)^4 = \frac{1}{6}\frac{E}{E_2}\left(1 + \frac{2h_a}{h}\frac{E_2}{E_a}\right), \tag{12}$$

which for the case when there is no adhesive layer, and again ignoring shear effects, reduces to

$$\left(\frac{\Delta}{h}\right)^4 = \frac{1}{6}. \tag{13}$$

It should be noted that G_c is given by the area under the stiffness curve (see Figure 4a), so that

$$G_c = \frac{\sigma_{\max}^2}{2}\left(\frac{b}{k_s}\right) \tag{14}$$

and

$$\sigma_{\max}^2 = 2G_c\left(\frac{k_s}{b}\right). \tag{15}$$

Combining the above equations yields, for the linear-elastic stiffness approach, the corresponding values of $\sigma_{\max}$ to be deduced for when the adhesive layer is absent, or can be ignored:

$$\sigma_{\max} = 2\left(\frac{G_c E}{h}\right)^{1/2}, \tag{16}$$

and with the adhesive layer included:

$$\sigma_{\max} = 2\left(\frac{\frac{G_c E}{h}}{1 + \frac{2h_a}{h}\frac{E_2}{E_a}}\right)^{1/2}. \tag{17}$$

It is very important to note that in the linear-elastic stiffness approach the term $\sigma_{\max}$ is not taken to be a material property and the fracture process is controlled by k_s and G_c. Indeed, any models which simply assume such an elastic-stiffness approach to describe a cohesive zone region at the crack tip do not make any assumptions of

a critical, limiting maximum value of the stress, σ_{max}, for the crack tip region. Thus, they all yield a *single* characteristic fracture parameter, namely G_c. However, the corresponding maximum value of the stress, σ_{max}, that results can be calculated from a knowledge of the value of G_c, as shown above in Equations (16) or (17) as appropriate, but the value so deduced is not considered to be a critical fracture parameter nor a material property. This linear elastic-stiffness approach is the form used in previous publications [1, 6] and is effectively the linear-elastic fracture-mechanics (LEFM) approach with a single characterising parameter, G_c.

The Critical, Limiting Maximum Stress, σ_{max}, Approach

On the other hand, recent cohesive zone models [4, 7] have been developed which propose a fracture criterion where *two* parameters must be used to describe the fracture process: namely G_c *and* σ_{max}, as shown in Figure 5. Here σ_{max} is assumed to be a critical, *limiting* maximum value of the stress in the damage zone ahead of the crack and is often assumed to have some physical significance. Such two-parameter models allow deviations from LEFM to be described.

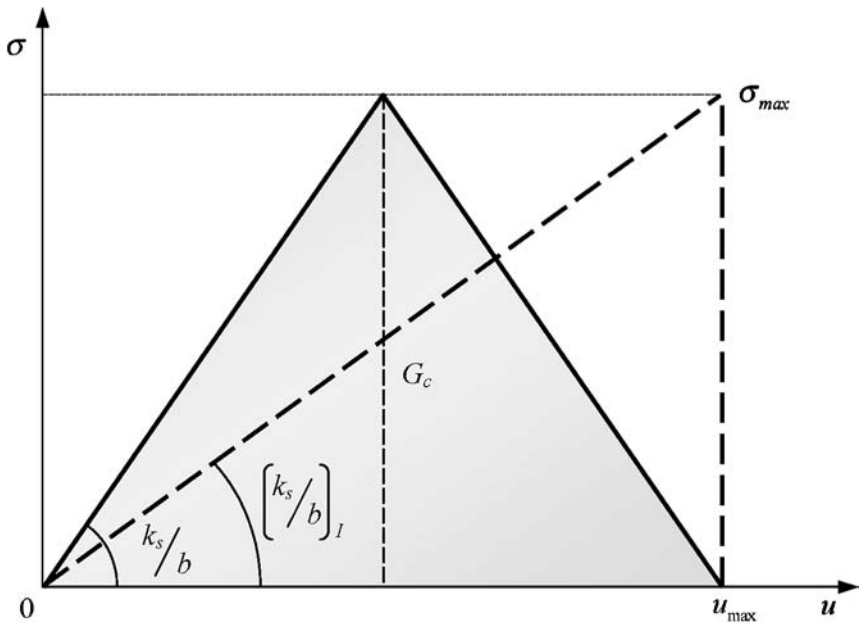

FIGURE 5 Critical, limiting maximum stress, σ_{max}, approach.

A recent study [6] showed that a two-parameter, cohesive zone model could be developed for different triangular forms of the stress *versus* displacement separation law which is taken to describe the physical characteristics of the cohesive zone. Hence, a critical value of $\sigma_{\max}$ value could be prescribed, as shown in Figure 5. Now, because the shape is not important, this is equivalent to the case shown in Figure 4 with a slope of $(k_s/b)_{\mathrm{I}}$, which is given by

$$\left(\frac{k_s}{b}\right)_I = \frac{\sigma_{\max}^2}{2G_c}, \tag{18}$$

and hence

$$\left(\frac{\Delta}{h}\right)^4 = \frac{2}{3}\frac{EG_c}{h\sigma_{\max}^2}. \tag{19}$$

Now, k_s/b is not a predetermined property, but the term $\sigma_{\max}$ is considered to be so in this critical, limiting maximum, $\sigma_{\max}$, approach.

It may be noted that when Equation (19) is used together with Equation (9), we have a relation between G and the $\sigma_{\max}$ of the form

$$\frac{G}{G_c} = \left(\frac{\sigma_{\max}}{\sigma_y}\right)^{1/4} \frac{3^{1/8}}{\varepsilon_y^{1/2}} \left(\left[\frac{\widehat{G}}{G_c}\right]^{5/4} \left[1 - \frac{\widehat{G}}{G_c}\right] \right)^{1/2}, \tag{20}$$

where

$$\widehat{G} = \frac{\sigma_y^2 h}{2E} \; and \; \varepsilon_y = \frac{\sigma_y}{E}. \tag{21}$$

(It also should be noted that the equivalent relationship to Equation (20) for the linear-elastic stiffness approach, using Equation (13), is

$$\frac{G}{G_c} = \frac{6^{\frac{1}{3}}}{\varepsilon_y^{1/2}} \left[\left(\frac{\widehat{G}}{G_c}\right) \left(1 - \frac{\widehat{G}}{G_c}\right) \right]^{1/2}, \tag{22}$$

where clearly the term $\sigma_{\max}$ is not involved.)

INCLUSION OF WORK-HARDENING EFFECTS

Theoretical

The above analyses all assume that the peel arm does not work-harden, *i.e.*, it is an elastic perfectly plastic material. However, the plastic bending may be modelled using large-displacement beam

theory modified for plastic bending [1, 3]. The formulation of this problem was given in detail in Kinloch et al. [1] for both linear and power-law work hardening for the peel arm but was then evaluated only for the former case. The power-law curve is taken to be of the form

$$\begin{aligned} \sigma &= \sigma_y \left(\frac{\varepsilon}{\varepsilon_y}\right)^N \quad \text{for } \varepsilon > \varepsilon_y, \\ \sigma &= E\varepsilon \qquad\quad \text{for } \varepsilon \leq \varepsilon_y, \end{aligned} \tag{23}$$

where ε_y is the yield strain and is given by $\varepsilon_y = \frac{\sigma_y}{E}$. The above is a very useful and accurate representation for fitting the stress *versus* strain curves of many materials.

A code, termed "ICPeel," was next developed to solve the above equations for the peel tests and, hence, deduce the value of G_d, and, hence, ascertain the value of the true adhesive fracture energy, G_c. This code was implemented using the commercially available "MathCad" mathematical software program. The "ICPeel" code can be used to deduce the value of G_c from the measured peel energy, G, using any form of the (Δ/h) relationship. Thus, it can be used with either (a) the simple linear-elastic stiffness approach (see Equation (12)) or (b) the critical, limiting maximum stress, $\sigma_{\max}$, approach (see Equation (19)). (Although, it should be noted that somewhat more accurate versions of these equations, which include shear effects and an extra correction for plasticity taken from Williams and Hadavania [9], are used in the "ICPeel" program; see Appendix A.) For the former, simple linear-elastic stiffness approach, the code also deduces the corresponding value of $\sigma_{\max}$ from Equation (16) or (17), as appropriate; while for the latter approach the value of $\sigma_{\max}$ is a required input parameter. Further, the code may be used with either a bilinear (see Kinloch et al. [1]), or the above power-law elastic-plastic material model to describe the stress *versus* strain relationship for the peel arm. Also, either a single-arm peel (for a given peel angle, θ,) or a T-peel test can be analysed. The code is available *via* our website [8]. The numerical algorithm implemented in the "ICPeel" code is outlined below, while all the equations used are listed in Appendix A for the different material models.

It is convenient in the peel analysis to introduce a nondimensional curvature variable, k, defined as

$$k = \frac{R_1}{R}, \tag{24}$$

where R is the current radius of curvature of the peeling arm and the subscript 1 denotes the condition for when the outer layers of

the substrate arms first reach the yield criteria, *i.e.*, $\sigma(h/2) = \pm\sigma_y$. In the peel test the substrate arm goes through bending and unbending cycles with the parameter k ranging from: (a) $0 < k < 1$ for pure elastic bending, (b) for elastic-plastic bending, (c) $k_{00} < k < k_0$ during elastic unbending, and (d) $0 < k < k_{00}$ during elastic-plastic unbending. The maximum value for k occurs at the end of the bending process, where $k = k_0$, at which stage the specimen arm exhibits the minimum radius of curvature. The term k_{00} represents the limiting value of the non-dimensional curvature during unbending, at which stage the outer layers of the substrate arms first start undergoing reverse plastic deformation. The corresponding bending stresses in the outer layers at $k = k_{00}$ are equal and opposite to the maximum stresses reached in the layer during bending at $k = k_0$. By knowing k_0, the whole bending and unbending history may be reconstructed analytically, *i.e.*, the moment-curvature diagram may be determined and, hence, the dissipated energy for plastic bending deduced. The core of the numerical algorithm obtains the unknown parameter k_0, such as to satisfy the global energy balance in the peel test. The easiest route is to calculate the value of k_0, *via* the *Area* [*OFABC*] from the moment diagram (see Figure 2b):

$$Area[OFABC] = P[1 - cos(\theta - \theta_o)] = \frac{E\varepsilon_y^2 bh}{2} \cdot f_2(k_0). \tag{25}$$

The function $f_2(k_0)$ is determined by direct integration of the moments resulting from the stress profiles in the arm cross-section during bending and unbending. It is specific to the assumed plastic hardening rule, and here we have used both a power-law rule and a linear-hardening rule. The local peel angle of the arm, θ_o, when $k = k_0$, remains the only unknown on the lefthand side of Equation (25). The general expression for the local peel angle, θ_0, from Equation (8) may now be rewritten to become

$$\theta_o = \frac{\Delta}{R} = \frac{\Delta}{R_1} k_0 = 2\left(\frac{\Delta}{h}\right)\varepsilon_y k_0. \tag{26}$$

If the linear-elastic stiffness approach is used for determining the characteristic deformation length, Δ (see Equation (12)), the function $\theta_0(k_0)$ is linear. In the critical, limiting maximum stress approach (see Equation (19)), the function is more complex and is described through $G_c(k_0)$. In either case, Equation (26) illustrates that θ_0 is solely a function of k_0 and, hence, the Newton-Raphson method, implemented in "Math-Cad" *via* its standard "*root*()" function, may be used to solve Equation (25) numerically. After k_0 has been found, all the other

dependent variables can be calculated explicitly, *e.g.*, the energy dissipated during the bending and unbending process is given by:

$$Area[OABC] = G_d b = \frac{E\varepsilon_y^2 bh}{2} \cdot f_1(k_0). \tag{27}$$

For both approaches, Equations (25) and (26) represent a closed, nonlinear numerical system. In the case of the linear-elastic stiffness approach, the solution for k_0 is obtained with a single "*root*()" function call, since $\theta_o(k_0)$ is a known function of k_0. However, in the critical, limiting maximum stress approach, the root rotation, θ_o, is also a function of the unknown variable G_c. This requires an iterative solution procedure. At the start of the calculation, G_c is initialised to G and is used to calculate a first estimate for $\theta_o(k_0, G_c)$. With the G_c specified, the corresponding k_0 can be obtained using the "*root*()" function. The calculated k_0 is now used to update G_d using Equation (27), from where the current G_c becomes $G_c = G - G_d$. This yields a new, improved estimate for $\theta_o(k_0, G_c)$. Within the iteration loop, k_0 gradually converges to a constant value and the rate of change of G_d and G_c decreases significantly. The calculation stops when changes in the adhesive fracture energy, G_c, are lower than a prescribed convergence tolerance, *i.e.*, $|\Delta G_c| < 0.001$. The computing algorithm is very efficient; the results are typically obtained within less than five iterations, for which the CPU time is on the order of a second.

The Effects of Work Hardening and σ_{max}

To illustrate the effects of both work hardening, and the use of $\sigma_{\max}$, some hypothetical peeling results, using a single-arm 90° peel test, of an aluminium-alloy strip bonded *via* an adhesive layer to a rigid substrate, were theoretically explored. The peel arm was taken to have the following values: $h = 1\,\text{mm}$, $E = 69\,\text{GPa}$, $\sigma_y = 84\,\text{MPa}$ and $N = 0.22$. The values of G_c were assumed to be in the range 700 to $1600\,\text{J/m}^2$, which is representative of a typical structural adhesive. The adhesive layer was assumed to have the values of $h_a = 0.4$ mm and $E_a = 3\,\text{GPa}$.

The linear elastic-stiffness approach (see Equation (12)) gives $\Delta/\text{h} = 1.4$ and, for $700 < G_c < 1600\,\text{J/m}^2$, these values in turn give from Equation (17) corresponding values of $90 < \sigma_{\max} < 140\,\text{MPa}$. A typical epoxy adhesive has a yield stress of about 50 MPa, so these values are sensible and indicate constraint factors, $\sigma_{\max}/\sigma_{ya}$, of 1.8 to 2.7, where σ_{ya} is the uniaxial tensile yield stress of the adhesive. However, for the linear elastic-stiffness approach, since the resulting

value of $\sigma_{\max}$ is now "fixed," no further exploration of the implications of using this approach can be undertaken.

On the other hand, for the purposes of exploring the alternative critical, limiting maximum stress, $\sigma_{\max}$, approach in detail, the values of $\sigma_{\max}$ may be varied more widely, keeping the value of G_c constant at a value of $700\,\mathrm{J/m^2}$ or $1600\,\mathrm{J/m^2}$. Equation (20) was used for when $N=0$ and the "ICPeel" analysis, described above, was used for when $N=0$ and $N=0.22$. Figure 6 shows G/G_c as a function of $\sigma_{\max}^{1/4}$, since Equation (20) indicates linearity in this form for $N=0$. This is confirmed, although the predictions of Equation (20) are somewhat different from the more accurate solutions (see the previous Theoretical section) from the "ICPeel" analysis, which are shown as the solid lines. As may be seen, from comparing the results for $N=0$ and $N=0.22$, there is only a slight effect of work hardening in this case. As expected, the measured peel force, $P/b=G$, continues to increase as the value of $\sigma_{\max}$ is increased, since more plasticity can be induced in the peel arm as the value of $\sigma_{\max}$ is increased.

Figure 7 shows a hypothetical case in which the value of the yield stress, σ_y, of the peeling arm is varied for constant values of $\sigma_{\max}$ and G_c. The relationship between G and σ_y was again explored by obtaining

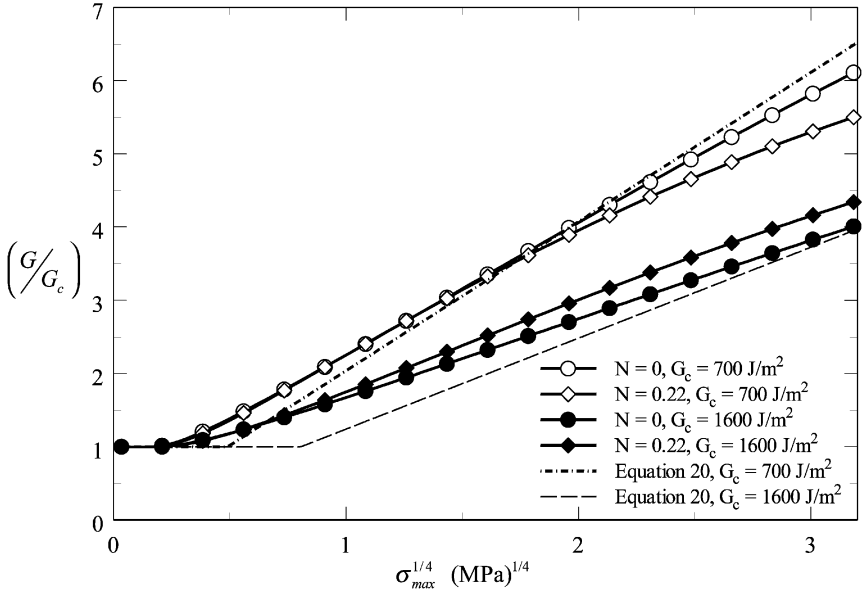

FIGURE 6 The effect of $\sigma_{\max}$ on total G for $\sigma_y=84\,\mathrm{MPa}$ as a function of $\sigma_{\max}$ as predicted from the critical, limiting maximum stress approach.

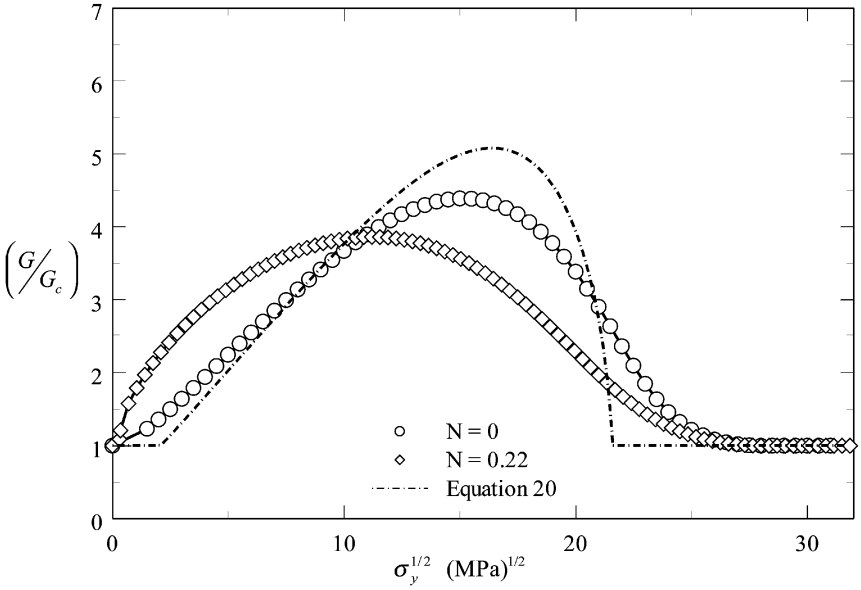

FIGURE 7 The effect of σ_y on total G for $\sigma_{max} = 50$ MPa and $G_c = 1600$ J/m^2 as predicted from the critical, limiting maximum stress approach.

predictions for this relationship by using Equation (20) (*i.e.*, for when $N = 0$) and the "ICPeel" analysis for when $N = 0$ and $N = 0.22$. At low σ_y values, $G \to G_c$ since the plastic work in the peel arm decreases; and at large σ_y values the system becomes increasingly elastic and again $G \to G_c$. Thus, there is a maximum in the measured peel force, $P/b = G$, as function of σ_y and there exists a range of relatively high values of σ_y where little variation in G may be observed. In this case, there is quite a marked effect of work hardening.

Finally, using the same methodology as before, a very similar situation pertains when the thickness, h, of the peel arm is varied for fixed values of $\sigma_{\max}$, σ_y, and G_c, as shown in Figure 8. Here, a non-dimensional measure of h (*i.e.*, $\hat{G}/G_c$) is plotted to the 5/8 power as suggested by Equations (20) and (21), and this approximate solution is very close to the computed results *via* the more accurate "ICPeel" analysis for $N = 0$. However, work hardening has a strong effect at relatively high thicknesses, since it increases the tendency to elastic behaviour. At low thicknesses, h, of the peel arm, there is only a slight effect and the computed values are lines with an intercept of unity. Such variations in h may well form the basis of a future experimental method of correcting G to find G_c.

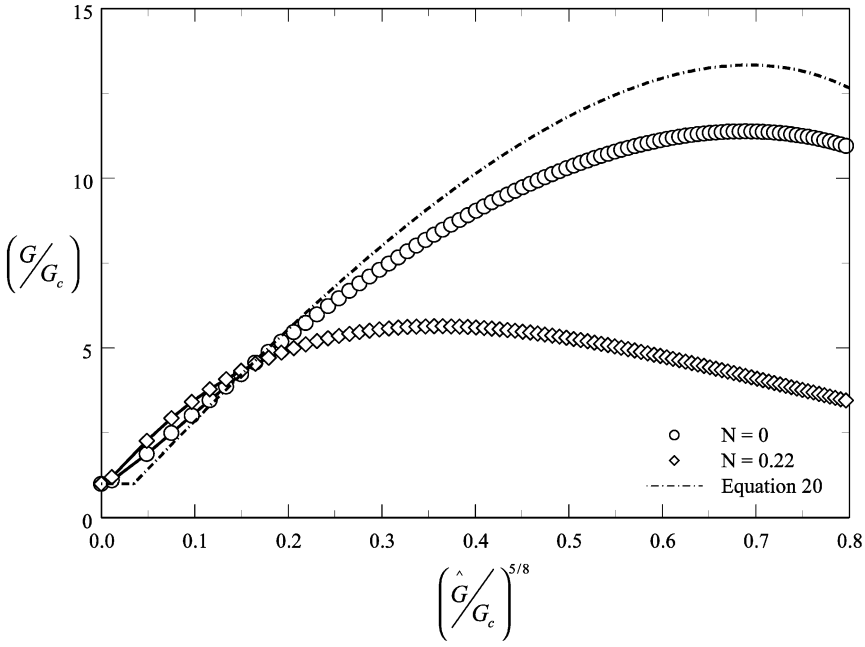

FIGURE 8 Thickness effects as predicted from the critical, limiting maximum stress approach; $\hat{G} = \frac{\sigma_y^2 h}{2E}$, $\sigma_{\max} = 50\,\text{MPa}$, $G_c = 1600\,\text{J/m}^2$.

The data used in Figures 6 to 8 clearly illustrate some of the complex relationships between G_c and the value of $\sigma_{\max}$ when the critical, limiting maximum stress, $\sigma_{\max}$, approach is adopted. Also, these results emphasise the crucial feature of this approach in that there are these *two* critical parameters, and to ascertain the true value of G_c requires the value of $\sigma_{\max}$ to be determined with some degree of accuracy.

EXPERIMENTAL EVIDENCE

Peeling of Polymeric Laminates

Introduction

An earlier paper [1] examined the peeling of thin polymer films of (a) polyethylene (PE) from aluminium-foil substrates, (b) poly(ethylene terephthalate) (PET) from aluminium-foil substrates, and (c) poly-(ethylene terephthalate) from polyethylene substrates. The polymers were all supplied by Du Pont (Wilmington, Delaware, USA). In the earlier paper the results were analysed *via* the linear-elastic stiffness

approach. However, both this approach and the critical, limiting maximum stress approach will now be considered in order to analyse the peeling process in order to assess the true, "characteristic," adhesive fracture energy, G_c. In these calculations the "ICPeel" code was used (see Appendix A) to solve the previous equations employing either (a) the simple linear-elastic stiffness approach or (b) the critical, limiting maximum stress, σ_{max}, approach; but the peeling arm was modelled as a bilinear elastic-plastic material, in accord with the earlier study [1].

Effect of Peel Arm Thickness, h

A set of values for a polyethylene (Grade PE1) substrate peeling away from the aluminiumfoil taken from the earlier paper [1] is given in Table 1, in which the thickness, h, varies from 30 μm to 215 μm for a peel angle of 180°.

First, the analysis of these results was performed on the basis of the linear-elastic stiffness approach, so no account was taken of the cohesive zone stress, σ_{max}. Thus, the G_c values are calculated using the value of Δ/h from Equation (13), which is the linear-elastic stiffness approach, with $E_2 = E$ and, since there was no adhesive layer, $\Delta/h = 0.64$. The analysis gives a sensibly constant value of G_c, as can be seen from Table 1. From Equation (16) the corresponding values of σ_{max} may be determined. They are not constant in value but vary systematically from 46.7 to 16.5 MPa. The yield stress of the polyethylene peel arm was approximately 7 MPa, giving a constraint factor, σ_{max}/σ_y, of between about 6.7 to 2.4. From the results shown in Table 1, it may also be seen that the value of G/G_c has a peak at about $h = 95$ μm, in agreement with the results shown earlier in Figure 8.

Second, these data have been reworked using Equation (19) to deduce the value of Δ/h, keeping σ_{max} constant, as a function of the

TABLE 1 180° Peel Test Results: Peeling an Aluminium Foil of Thickness h from a Polyethylene Substrate (Grade PE1)

h (μm)	G (J/m)^2	G_c (J/m)^2	σ_{max} (MPa)
30	195	81.1	46.7
45	205	72.3	36.0
60	240	80.2	32.8
75	260	82.4	29.7
105	260	75.7	24.1
135	225	65.1	19.7
165	240	71.0	18.6
215	220	72.8	16.5

thickness, h, of the peel arm. Thus, we now impose the condition that for all values of h the value of the stress, σ_{max}, must reach a critical, limiting maximum value for the peel process to occur. The value of G_c as a function of h is shown in Figure 9 for a range of constant σ_{max} values. Employing a low σ_{max} value, *e.g.*, 15 MPa, clearly gives a substantial variation in G_c; but for $\sigma_{max} = 45$ MPa the value of G_c is almost as constant as the value of G_c computed from the linear-elastic stiffness approach. However, it is noteworthy that the linear-elastic stiffness approach, where the corresponding value of σ_{max} was not constant, see Table 1, marginally gave the least variation in G_c as a function of h.

Effect of Peel Angle, θ

There are also four sets of data in the earlier paper [1] in which the peel angle was varied for polyethylene films (using two grades of different molecular weight: PE1 and PE2) peeling away from an aluminium foil and for a poly(ethylene terephthalate) (PET) film peeling away from a polyethylene substrate (using two different commercial tie-layer adhesives supplied by Du Pont, Wilmington, Delaware, USA, to change the level of adhesion at the PET/PE1 interface: T1 and T2).

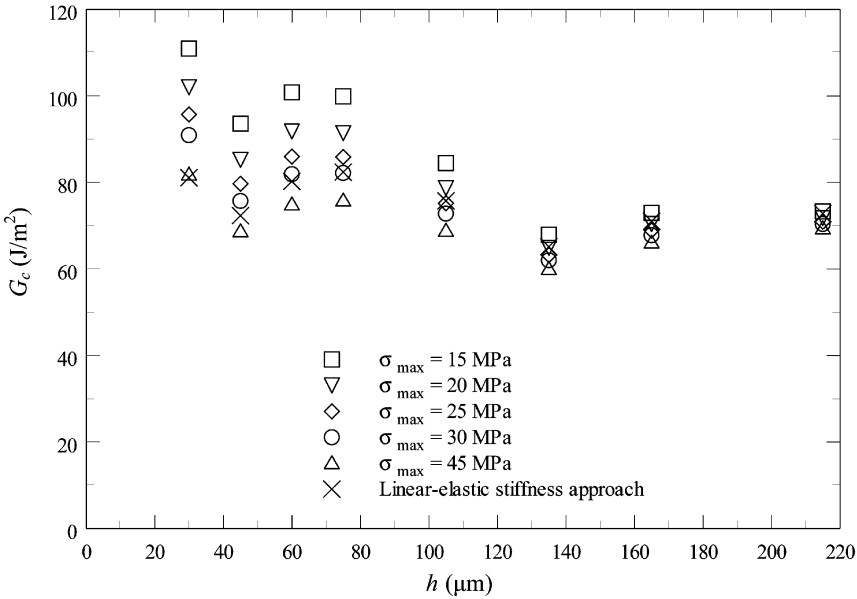

FIGURE 9 Results for the PE1/A1-foil laminates with various thicknesses h of PE1 (the peeling arm) with $\theta = 180°$.

In all cases the substrate film was rigidly supported. It should be noted that the two different grades of polyethylene differed with respect to their molecular weight, molecular weight distribution, and degree of orientation, and this led [1] to different mechanical properties for the two polyethylene films.

First, in general the linear-elastic stiffness approach, *i.e.*, with Δ/h being ascertained *via* Equation (13), gave constant values of G_c. In all these sets of test specimens the value of h was constant, so for each set of test specimens the corresponding values of σ_{max} are proportional to $\sqrt{G_c}$ (see Equation (16)). Hence, the corresponding value of σ_{max} was also reasonably constant. Second, to explore the usefulness of the critical, limiting maximum stress, σ_{max}, approach for these different sets of peel test results, the values of σ_{max} were varied relatively widely, and the variation in G_c with the peel angle, θ, noted. Again, Equation (19) was employed to deduce the value of Δ/h, keeping σ_{max} constant. Thus, we now again impose the condition that the stress, σ_{max}, must reach a critical, limiting maximum value for the peel process to occur, whatever the peel angle.

The results from both approaches are shown in the form of G_c as a function of θ in Figures 10a to 10d. For the polyethylene (PE1) results, shown in Figure 10a, the most constant value of G_c as a function of the applied peel angle, θ, came from using the critical, limiting maximum stress, σ_{max}, approach when using a σ_{max} value of 30 MPa. The linear-elastic stiffness approach yielded a less constant value of G_c with θ and gave a significantly higher value for the resulting σ_{max} of 60 MPa. On the other hand, for the other polyethylene (PE2) laminate (see Figure 10b), both approaches gave an equally good constant value of G_c as a function of the applied peel angle, θ. Further, the value of $\sigma_{max} \approx 100$ MPa, which was obtained using the linear-elastic stiffness approach, was also the optimum value required to be employed in the critical, limiting maximum, σ_{max}, approach. However, this value of σ_{max} does lead to a relatively high constraint factor, σ_{max}/σ_y, of about 9.

In Figures 10c and 10d, the two poly(ethylene terephthalate) (PET) sets of data are for different surface treatments (T1 and T2) and G_c changes, although the bulk properties of the polymer film do not. The data in these show more variation of G_c with θ than was seen for in the results for the polyethylene laminates, but the linear-elastic stiffness approach and, the critical, limiting maximum stress, σ_{max}, approach both yield sensible fits to the data, with approximately the same value of σ_{max} being implied or required, respectively. From Figure 10c, we have $G_c \approx 50\,J/m^2$ and $\sigma_{max} \approx 400$ MPa and, from Figure 10d, we have $G_c \approx 30\,J/m^2$ and $\sigma_{max} \approx 300$ MPa. Now, since for the PET peeling arm

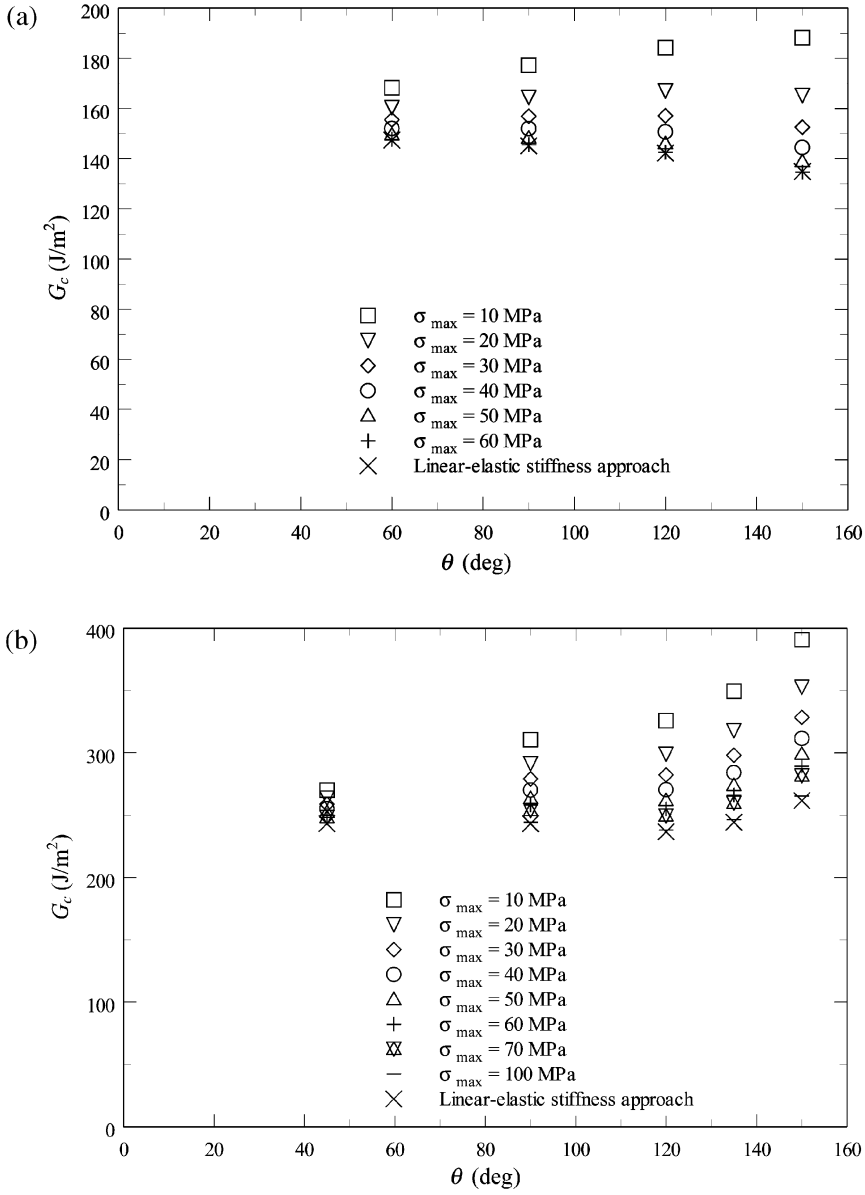

FIGURE 10 (a) Results for the PE1/A1-foil laminates. (b) Results for the PE2/A1-foil laminates. (c) Results for the PET/T1/PE1 laminates. (d) Results for the PET/T2/PE1 laminates.

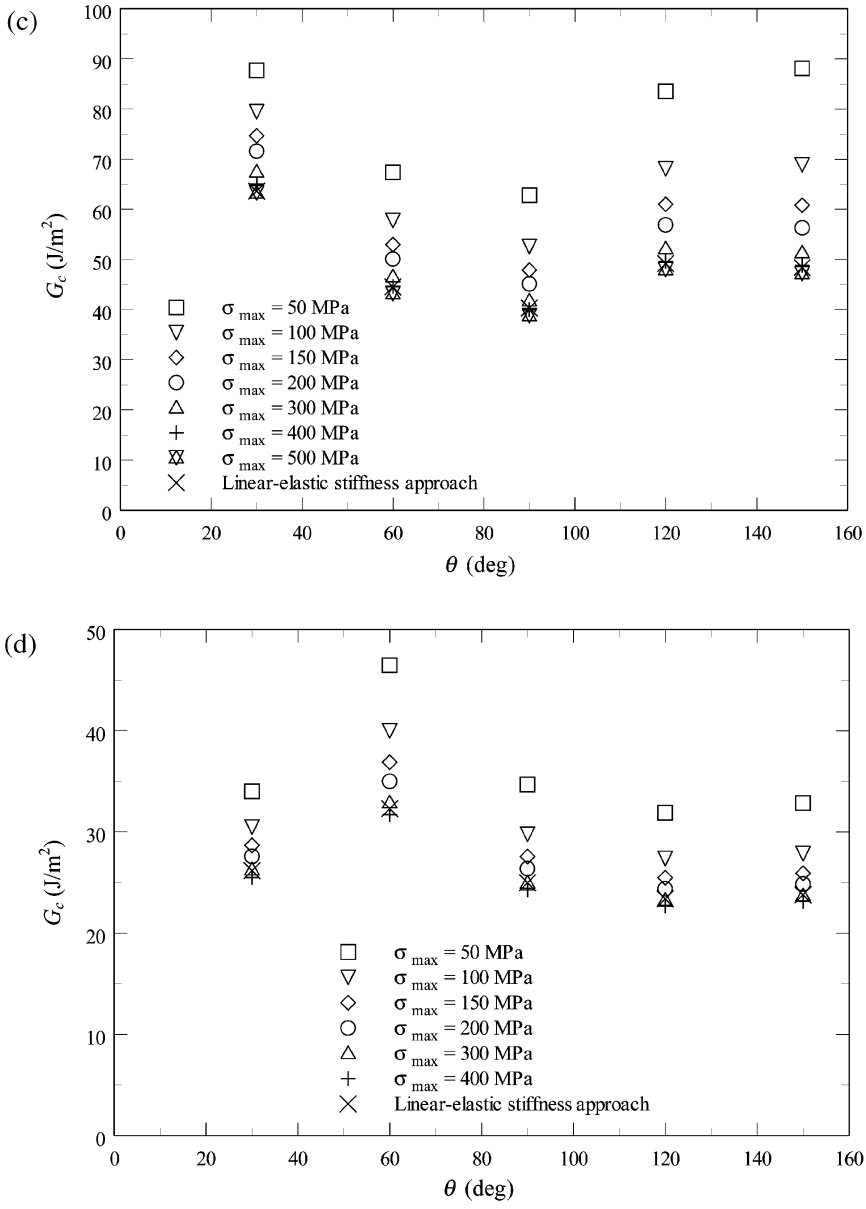

FIGURE 10 Continued.

$\sigma_y = 91\,\text{MPa}$, these values of $\sigma_{\max}$ correspond to constraint factors of about 4.4 and 3.4, respectively.

Peeling of Aluminium-Alloy Epoxy-Bonded T-Peel Test Specimens

There are also some experimental data available on peeling apart aluminium alloy strips which were bonded using a relatively tough epoxy adhesive [10], employing the T-peel test. Aluminium alloy (ISO Grade 5754: a general purpose, 2.6 to 3.6 w/w% magnesium, aluminium alloy) gave constant G ($=2P/b$) values of $16.8\,\text{kJ/m}^2$ and $20.8\,\text{kJ/m}^2$ for $h = 1$ and 2 mm, respectively.

The linear-elastic stiffness approach using the "ICPeel" program was used to deduce the values of G_c and the resulting $\sigma_{\max}$ values. Taking the aluminium alloy arms to be a power-law hardening material with $E = 66$ GPa, $\sigma_y = 85$ MPa, and $N = 0.22$ gave G_c values of $3.2\,\text{kJ/m}^2$ and $3.4\,\text{kJ/m}^2$, respectively, with corresponding values of $\sigma_{\max}$, *via* Equation (17), of 290 MPa for both thicknesses of the peel arms. If instead the arms are modelled as a bilinear work-hardening material with $E = 66\,\text{GPa}$, $\sigma_y = 130\,\text{MPa}$, and with the hardening coefficient, $\alpha = 0.011$, the analysis now gave G_c values of $3.1\,\text{kJ/m}^2$ and $3.0\,\text{kJ/m}^2$, respectively, with corresponding values of $\sigma_{\max}$, *via* Equation (17), of 285 MPa and 270 MPa.

The consistency of G_c is, therefore, good and, indeed, a linear-elastic fracture-mechanics test (LEFM) based upon a tapered-double cantilever-beam joint, using the same adhesive, gave a value $G_c = 2.7 \pm 0.4\,\text{kJ/m}^2$. (In all these tests the locus of joint failure was cohesive in the adhesive layer.) Considering the resulting values of $\sigma_{\max}$, they then represent constraint factors of about 5.5 to 6, when compared with the yield stress, σ_{ya}, of the adhesive, which was approximately 50 MPa.

CONCLUSIONS

The analytical methods given here show that it is possible to develop an elastic-plastic model of the peeling test by adopting either (a) a linear-elastic stiffness approach or (b) a critical, limiting maximum stress, $\sigma_{\max}$, approach in order to assess the true, "characteristic" adhesive fracture energy, G_c.

It is very important to note that in the linear-elastic stiffness approach the term $\sigma_{\max}$ is not taken to be a material property and that the fracture process is controlled by k_s and G_c. Indeed, any models which simply assume such an elastic-stiffness approach to describe a cohesive zone region at the crack tip do not make any assumptions of a

critical, limiting maximum value of the stress, σ_{max}, for the crack tip region. Thus, they all yield a *single* characteristic fracture parameter, namely G_c. However, the corresponding maximum value of the stress, σ_{max}, that results can be calculated from a knowledge of the value of G_c. On the other hand, recent cohesive zone models have been developed which propose a fracture criterion where *two* parameters are required to describe the fracture process: namely, G_c and σ_{max}. Here σ_{max} is assumed to be a critical, *limiting* maximum value of the stress in the damage zone ahead of the crack and is often assumed to have some physical significance.

Analysis of the peeling of polymer films clearly reveals that both the linear-elastic stiffness and the critical, limiting maximum stress, σ_{max}, approaches give quite accurate descriptions of the relationship of G with variations in the thickness of the peel arm and the peel angle, assuming a constant value of G_c. Indeed, they both yield values of G_c which are independent of these joint parameters. However, the T-peel tests on the aluminium alloy/toughened-epoxy provides a more valuable insight into the problem, since the value of G_c is known *a priori via* a standard LEFM test. Using the T-peel test results, the value of G_c obtained from the linear-elastic stiffness approach was (a) independent of thickness of the peel arm and (b) in good agreement with the value from the established LEFM tests. Also, it was noteworthy that the resulting value of σ_{max} was a function of the geometry of the peel test and not, therefore, a characteristic material parameter.

The need to know the value of σ_{max} in order to use the critical, limiting maximum stress, σ_{max}, approach is clearly a major obstacle. If the value of σ_{max} is assumed to be the stress which acts in the damage zone ahead of the crack and to have some physical significance, then it is more likely that some value might be attached to the σ_{max} term. Thus, a failure analysis of the peel test might then be more readily undertaken using this two-parameter approach. However, the present work has revealed no clear pattern as to any physical significance of the term σ_{max}. Indeed, we have found only that it is typically far greater in value than the yield stress of the peeling arm or adhesive layer when present. A crucial factor which we have considered in this respect is the constraint factor, m, by which the yield stress is elevated for an elastic system with full lateral constraint this is given by

$$m = \left(\frac{1-v}{1-2v}\right), \tag{28}$$

where v is Poisson's Ratio. For the stiffer polymers, $v \cong 0.35$ to 0.4 so that the maximum value of m prior to general yielding is typically 2.2 to 3. However, we have found that the values of σ_{max} for the relatively stiff

PET laminates gave constraint factors of about $m = 3.5$ to 4.5; and for the epoxy adhesive in the T-peel test, constraint factors of about $m = 5.5$ to 6 were ascertained. Thus, the experimental results are relatively high compared with those expected from Equation (28). For the softer materials, such as polyethylene, v can be as high as 0.45, giving $m = 5.5$ from Equation (28). However, for the polyethylene laminates the present work has again shown that the values of $\sigma_{\max}$ deduced lead to constraint factors significantly higher than expected, *i.e.*, up to $m = 9$.

In summary, either (a) a simple linear-elastic stiffness approach or (b) a critical, limiting maximum stress, $\sigma_{\max}$, approach can be used in an analytical elastic-plastic model of the peel test. Both give values of the adhesive fracture energy, G_c, which are independent of the details of the test geometry. However, the need to know an accurate value of $\sigma_{\max}$ in order to use the latter approach is clearly a major obstacle to employing the critical, limiting maximum stress, $\sigma_{\max}$, approach. This is especially relevant when it appears that little physical significance can be readily attached to the meaning of the $\sigma_{\max}$ term. Thus, the main conclusion is that the former approach, *i.e.*, the simple linear-elastic stiffness approach, is the preferred option in undertaking analytical modelling of the peel test. However, both approaches are implemented in the "ICPeel" code of the analytical elastic-plastic peel model, which can be downloaded from our website [8] for other workers to use and explore.

REFERENCES

[1] Kinloch, A. J., Lau, C. C., and Williams, J. G., *Int. J. Fract.*, **66**, 45–70 (1994).
[2] Kendall, K., *J. Adhesion*, **5**, 105–117 (1969).
[3] Kim, K. S., and Aravas, N., *Int. J. Solids and Struct.*, **24**, 417–435 (1988).
[4] Wei, Y., and Hutchinson, J. W., *Int. J. Fract.*, **93**, 315–333 (1998).
[5] Kanninen, M. F., *Int. J. Fract.*, **10**, 415–430 (1974).
[6] Williams, J. G., and Hadavinia, H., *J. Mech. Phys. Solids*, **50**, 809–825 (2002).
[7] Tvergaard, V., and Hutchinson, J. W., *J. Mech. Phys. Solids*, **41**, 1119–1135 (1993).
[8] Adhesion, Adhesives and Composites Group, Imperial College, London, website: http://www.me.imperial.ac.uk/AACgroup/index.html (2003).
[9] Williams, J. G., and Hadavinia, H., In: *14th European Conference on Fracture—ECF14*, Cracow, Poland, EMAS Publishing, **3**, 573–592 (2002).
[10] Georgiou, I., Ivankovic, A., Kinloch, A. J., and Tropsa, V., in 3rd ESIS TC4 Conference on the Fracture of Polymers, Composites, and Adhesives, Les Diablerets, Switzerland, Elsevier, *to be published*.

APPENDIX A (SEE FIGURE A1)

A.1 Equation (*)

For the linear-elastic stiffness approach, for the local peel angle, θ_0, the relevant equation is given by

$$\theta_0(k_0) = \sqrt{0.2 + \sqrt{0.058 + \frac{1}{3}\frac{h_a}{h}\frac{E}{E_a}}} \cdot \begin{cases} 2\varepsilon_y k_0 & \text{for} \quad k_0 < 1 \\ 2\varepsilon_y \frac{6k_0^3}{1+5k_0^2} & \text{for} \quad k_0 < 1, \end{cases}$$

whereas for the critical, limiting maximum stress case for θ_0 the relevant equation is given by

$$\theta_0(k_0, G_c) = \sqrt{0.2 + \frac{1}{\sigma_{\max}}\sqrt{\frac{2}{3}\frac{EG_c}{h}}} \cdot \begin{cases} 2\varepsilon_y k_0 & \text{for} \quad k_0 < 1 \\ 2\varepsilon_y \frac{6k_0^3}{1+5k_0^2} & \text{for} \quad k_0 > 1. \end{cases}$$

In the linear-elastic stiffness approach the maximum stress, $\sigma_{\max}$, is not a priori prescribed but merely is a consequence of the analysis. It may be calculated from

$$\sigma_{\max} = \frac{1}{\sqrt{0.058 + \frac{1}{3}\frac{h_a}{h}\frac{E}{E_a}}}\sqrt{\frac{2}{3}\frac{EG_c}{h}}.$$

A.2 Power-Law Hardening Material Model

The auxiliary functions, $f_1(k_0)$ and $f_2(k_0)$ used in the program are given as follows:

$$(**) \qquad f_2(k_0) = \begin{cases} f_{2e}(k_0) & \text{for} \quad k_0 < 2^{\frac{1}{1-N}} \\ f_{2ep}(k_0) & \text{for} \quad k_0 > 2^{\frac{1}{1-N}}, \end{cases}$$

where

$$f_{2e}(k_0) = \frac{k_0^2}{3},$$

and

$$f_{2ep}(k_0) = \frac{2}{2+N}k_0^{1+N} + \frac{2^{1-N}}{(2+2N-N^2)(1+N)}k_0^{2-(1-N)^2} \cdots + \frac{8}{3}\frac{(1-N)^2(4+N-2N^2)2^{\frac{3N}{1-N}}}{(1+2N)(2+N)(2+2N-N^2)}\frac{1}{k_0} - \frac{4}{(1+2N)(1+N)}k_0^{2N}$$

$$(***) \qquad f_1(k_0) = \begin{cases} 0 & \text{for} \quad 0 < k_0 < 1 \\ f_{1e}(k_0) & \text{for} \quad 1 < k_0 < 2^{\frac{1}{1-N}}, \\ f_{1ep}(k_0) & \text{for} \quad k_0 > 2^{\frac{1}{1-N}} \end{cases}$$

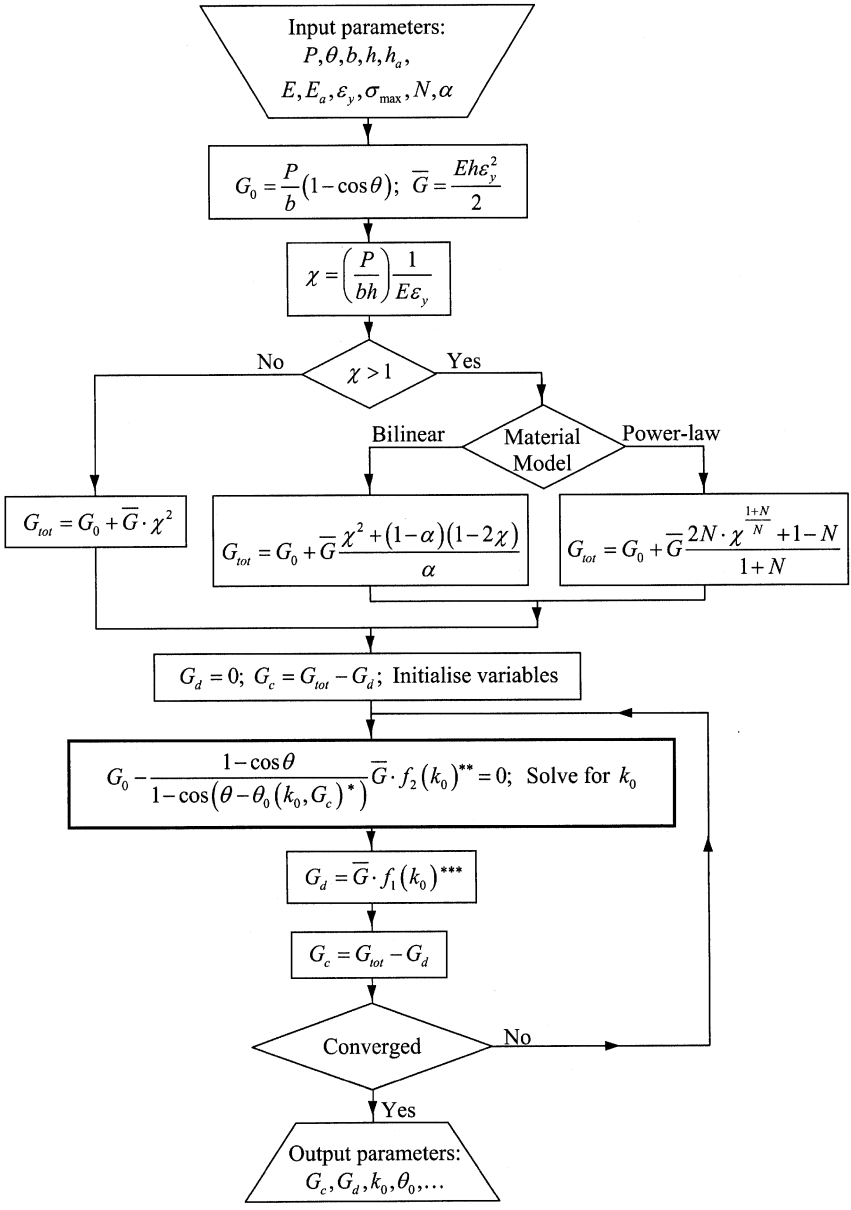

FIGURE A1 Block diagram of the peel algorithm implemented in "ICPeel". Note that the (*), (**), and (***) equations are listed on the following page.

where

$$f_{1e}(k_0) = \frac{k_0^2}{3} - \frac{2N}{(1+N)(2+N)} k_0^{(1+N)} + \frac{4}{3}\frac{(1-N)}{(2+N)}\frac{1}{k_0} - \frac{(1-N)}{(1+N)},$$

and

$$f_{1ep}(k_0) = \frac{2}{(1+N)(2+N)} k_0^{1+N} + \frac{2^{1-N}}{(2+2N-N^2)(1+N)} k_0^{2-(1-N)^2} \cdots + \left[\frac{1}{3}\frac{2^{\frac{3}{1-N}}(4+N-2N^2)(1-N)^2}{(1+2N)(2+N)(2+2N-N^2)} + \frac{4}{3}\frac{(1-N)}{(2+N)}\right]\frac{1}{k_0} - \frac{4}{(1+2N)(1+N)} k_0^{2N}\left(\frac{1-N}{1+N}\right).$$

The limiting value for the nondimensional curvature during unbending, k_{00}, (see above) for a power-law hardening material can be obtained from

$$k_{00} = k_0 - 2k_0^N.$$

If $k_{00} \leq 0$, then the substrate arms are still unbending elastically at the end of the peeling process. Therefore, the maximum value of k_0 that would guarantee elastic unbending at the end of the process ($k_{00} = 0$) is given by

$$k_0 = 2^{\frac{1}{1-N}}.$$

This limiting value for k_0 has been used as a switch in the functions $f_1(k_0)$ and $f_2(k_0)$ to ensure that the end of peel process is properly assessed, either as elastic or elastic-plastic unbending.

A.3 Bilinear Work-Hardening Material Model

The auxiliary functions $f_1(k_0)$ and $f_2(k_0)$ are given as follows:

$$(**) \qquad f_2(k_0) = \begin{cases} f_{2e}(k_0) & \text{for} \quad k_0 < 2\frac{(1-\alpha)}{(1-2\alpha)} \\ f_{2ep}(k_0) & \text{for} \quad k_0 > 2\frac{(1-\alpha)}{(1-2\alpha)}, \end{cases}$$

where

$$f_{2e}(k_0) = \frac{k_0^2}{3},$$

and

$$f_{2ep}(k_0) = \frac{1}{6}\alpha(3-2\alpha)^2 k_0^2 + 2(1-\alpha)\Big(1-\frac{\alpha}{2}\Big)(1-2\alpha)k_0 \ldots + \frac{8}{3}\frac{(1-\alpha)^3\big(1-\frac{\alpha}{2}\big)}{(1-2\alpha)k_0} - 4(1-\alpha)^2\Big(1-\frac{\alpha}{2}\Big),$$

$$(***) \qquad f_1(k_0) = \begin{cases} 0 & \text{for} \quad 0 < k_0 < 1 \\ f_{1e}(k_0) & \text{for} \quad 1 < k_0 < 2\frac{(1-\alpha)}{(1-2\alpha)} \\ f_{1ep}(k_0) & \text{for} \quad k_0 > 2\frac{(1-\alpha)}{(1-2\alpha)}, \end{cases}$$

where

$$f_{1e}(k_0) = (1-\alpha)\left[\frac{1}{3}k_0^2 + \frac{2}{3k_0} - 1\right],$$

and

$$f_{1ep}(k_0) = \frac{4}{3}\alpha\left[(1-\alpha)\Big(1-\frac{\alpha}{2}\Big) - \frac{1}{8}\right]k_0^2 + 2(1-\alpha)\Big(1-\frac{\alpha}{2}\Big)(1-2\alpha)k_0 \ldots + \frac{2}{3}\frac{(1-\alpha)}{(1-2\alpha)k_0}[1-2\alpha^2(2-\alpha)+4(1-\alpha)^3] - (1-\alpha)[1+2\alpha(1-\alpha)+4(1-\alpha)^2].$$

Reverse plastic bending will commence at

$$k_{00} = (1-2\alpha)k_0 - 2(1-\alpha).$$

At the end of the peel test, specimen arms are unbending elastically only if

$$k_0 = 2\frac{(1-\alpha)}{(1-2\alpha)},$$

the value of which is used as a switch in the terms $f_1(k_0)$ and $f_2(k_0)$.